Electronic Excitation Energy Transfer of Prodan-ORB and Laurdan-ORB Systems in Model Phospholipid Membranes

Katarzyna A. Kozyra, Marek Józefowicz, Janina R. Heldt, and Józef Heldt

Institute of Experimental Physics, University of Gdańsk, ul. Wita Stwosza 57, 80-952 Gdańsk, Poland

Reprint requests to M. J.; Fax: +48-583-413-175; E-mail: fizmj@univ.gda.pl

Z. Naturforsch. **63a,** 819 – 829 (2008); received May 13, 2008

Electronic energy transfer between prodan (6-propionyl-2-dimethylaminonaphthalene) and laurdan (6-dodecanoyl-2-dimethylaminonaphthalene) acting as donors and ORB (octadecyl rhodamine B) acting as acceptor in a model system of membranes has been studied by a steady-state fluorescence quenching analysis. Factors determining the energy transfer rate were considered with special attention to the contribution from the spectral heterogeneity of the donor molecules. By analyzing experimental data within the framework of two theoretical models (developed by Stern, Volmer, and Lehrer) of the energy transfer in two-dimensional systems, the limits of the range of possible prodan and laurdan positions with respect to a lipid bilayer have been estimated.

Key words: Fluorescence Quenching; Resonance Energy Transfer; Phospholipid Vesicles; Distance Estimation in Membrane.

1. Introduction

In the last several decades, a number of studies have demonstrated the utility of the excitation energy transfer as a technique for probing biological systems, especially for determining the spatial extension and geometrical characteristics of different compartments of living cells and their respective parts [1 – 3]. The benefits of the energy transfer are becoming increasingly evident to researchers who require measurements with high sensitivity, specificity, non-invasiveness, rapidity, and relative simplicity [3, 4].

The non-radiative transfer of electronic energy occurs without the emission of photons at distances shorter than the wavelength and results from short- or long-range dipole-dipole interactions between donor (D) and acceptor (A) molecules [4]. The quenching of donor fluorescence requires a close approach of a fluorophore and a quencher and, in the simplest case, is modeled based on the Stern-Volmer theory [5], which can be applied successfully to a wide variety of quenching studies in isotropic and low-viscosity solutions. For anisotropic systems such as phospholipid membranes, the deviation from linearity in the Stern-Volmer curve is observed [6]. This deviation generally falls into two categories: saturated and superlinear. The accurate description of the quenching process in such cases requires additional considerations. In certain cases, the saturated behaviour is characterized by the existence of an inaccessible fraction of fluorophores [7].

The efficiency of the energy transfer is governed by numerous factors including the distance between chromophores employed as the energy donor and acceptor, the donor quantum yield, overlap of the donor emission and acceptor absorption spectra, and relative orientation of the donor and acceptor transition moments [4]. Otherwise, an adequate description of the resonance energy transfer in membranes requires consideration of the geometry and dimensionality of the system being examined [8]. The theoretical background for the description of an energy transfer in membrane systems is provided by a number of models [9 – 13], in which such factors as the mode of the acceptor bilayer distribution, the curvature of lipid-water interface, the extent of area exclusion around the fluorophore could significantly contribute to the energy transfer efficiency for a given acceptor surface density.

A number of previous investigations reported by us [6, 14 – 16] and also by other groups [8, 17 – 19] have presented perspectives illustrating the influence of the phase transition on photophysics of various environmentally sensitive probes used as donors and acceptors in the energy transfer experiment. In contrast to our previous work [20], which relied on fluorescence quenching and energy transfer in an isotropic

0932–0784 / 08 / 1200–0819 $ 06.00

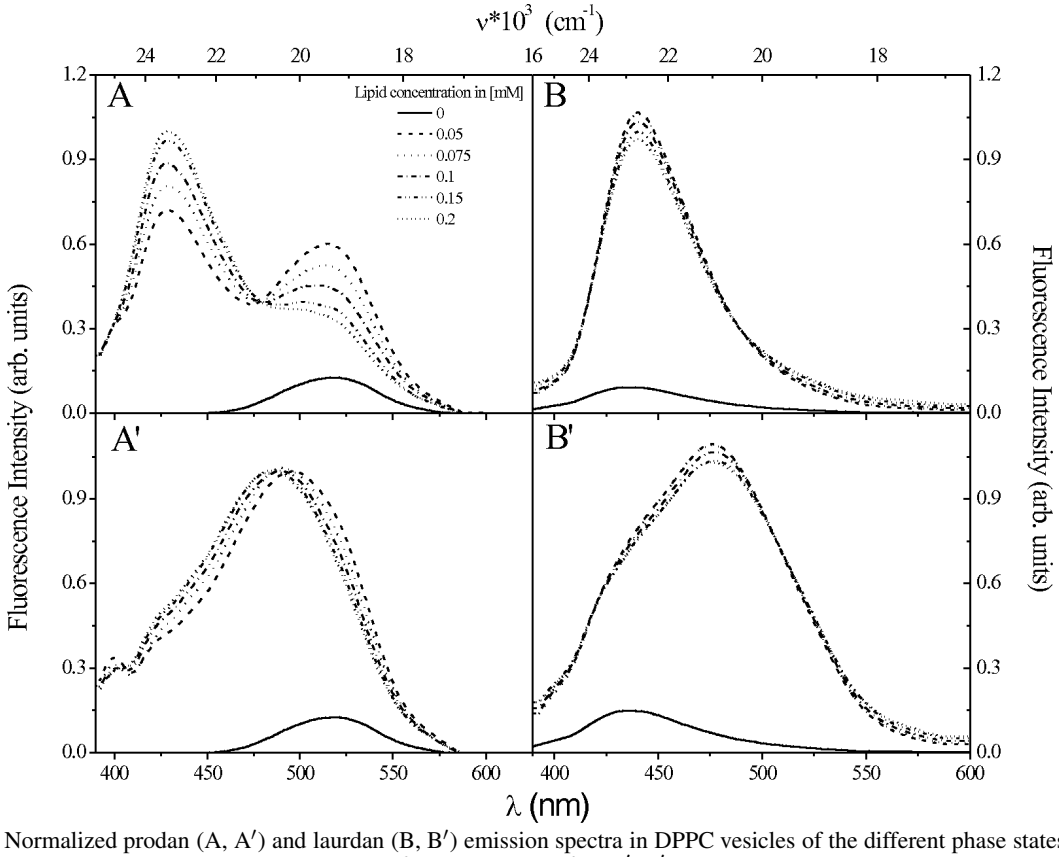

Fig. 1. Normalized prodan (A, A′) and laurdan (B, B′) emission spectra in DPPC vesicles of the different phase states in the presence of various concentrations of lipid at 25 °C (A, B) and 50 °C (A′, B′).

system, we here include fluorescence quenching in a lipid bilayer with the aim of obtain better insights into the distribution and localization of prodan and laurdan in SUVs (small unilamellar vesicles). In the present paper, fluorescence quenching and resonance excitation energy transfer have been used to determine the localization of prodan (6-propionyl-2-dimethylaminonaphthalene) and laurdan (6-dodecanoyl-2-dimethylaminonaphthalene) in vesicles composed of DPPC (1,2-dipalmitoyl-sn-glycero-3-phosphocholine). On the basis of experimental data (spectral fluorescence measurements) and theoretical calculations [analysis of the results of luminescence quenching of prodan and laurdan by incorporated ORB (octadecyl rhodamine B) molecules], quantitative interpretation of the results was performed in terms of two independent models. One of the applied models (based on the Stern-Volmer theory) takes into account the spectroscopic heterogeneity of prodan and laurdan incorporated into a bilayer. The other one considers the partition of the quencher between the aqueous phase and the above type of subphases (membranes or micelles). The result of this phenomenon is that the local concentration of fluorophores in the subphase may be much different from the overall concentration of the solution. The models mentioned above allow to evaluate of the main parameters describing the electronic excitation energy transfer.

2. Materials and Methods

Prodan, laurdan and ORB were purchased from Molecular Probes (Eugene, OR, USA). High-purity DPPC was purchased from Lipoid KG (Ludwigshafen, Germany) and used without further purification. SUVs composed of DPPC were prepared by sonication and extrusion methods [21].

Measurements of the fluorescence quenching of prodan and laurdan by ORB in SUVs prepared from DPPC

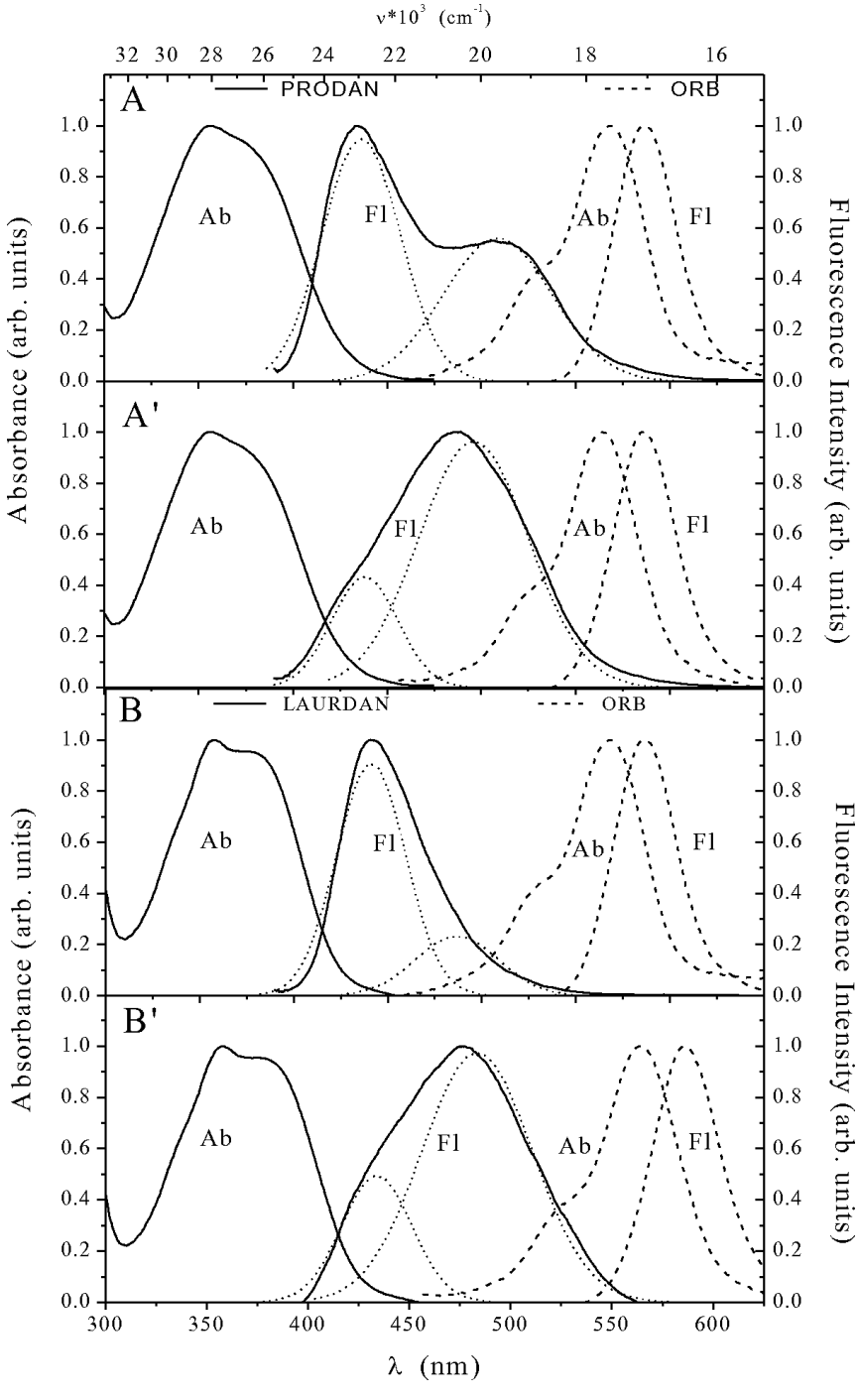

Fig. 2. Absorption (Ab) and fluorescence (Fl) spectra of prodan (A, A′), laurdan (B, B′), and ORB (A, A′, B, B′) in DPPC vesicles ([L] = 0.1 mM) at 25 °C (A, B) and 50 °C (A′, B′).

were carried out in a computer-controlled Perkin Elmer LS-50 spectrofluorimeter equipped with a thermostated cuvette (Julabo Labortechnik, Seelbach, Germany). The measurements were performed for both phases of the membrane, i. e., gel (25 °C) and liquid-crystalline phase (50 °C). The experimental procedures of the performed measurements have been described in details elsewhere [6, 14].

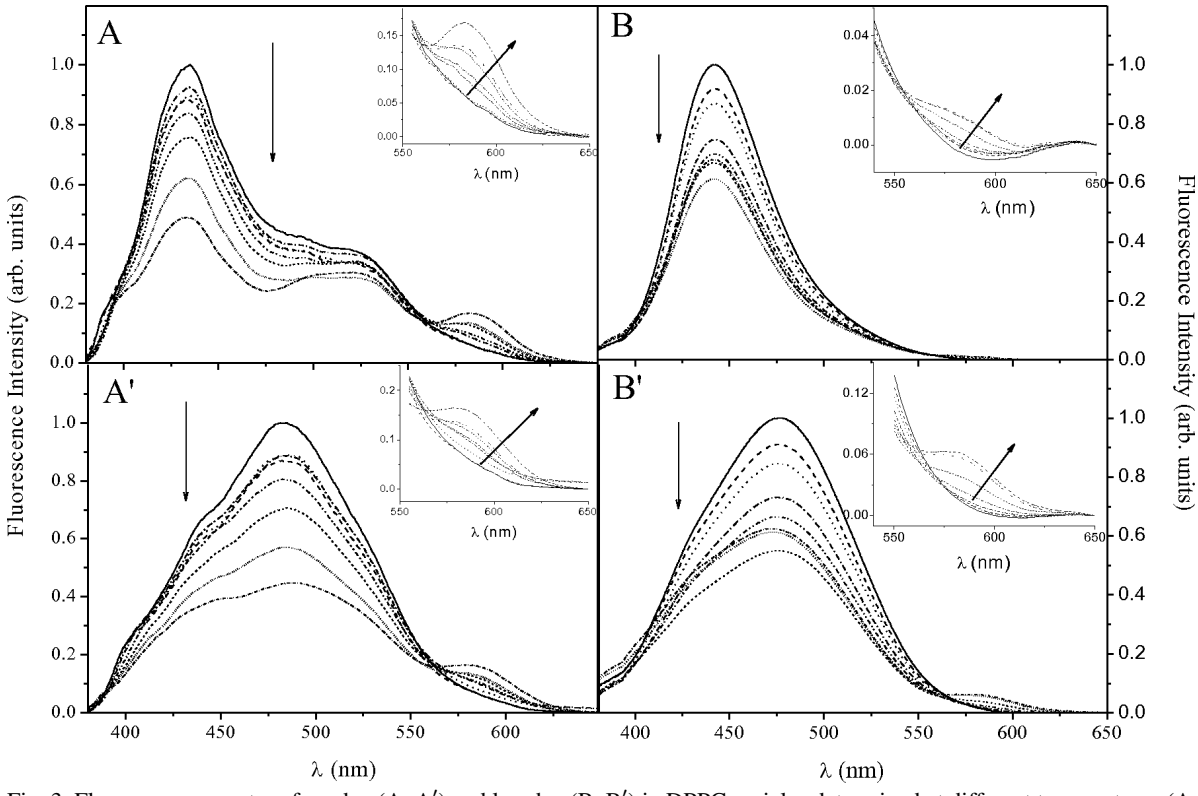

Fig. 3. Fluorescence spectra of prodan (A, A′) and laurdan (B, B′) in DPPC vesicles determined at different temperatures (A, B – 25 °C; A′, B′ – 50 °C) as a function of the ORB concentration.

3. Results and Discussion

3.1. Emission Spectra of Prodan and Laurdan

Figure 1 shows the emission spectra of prodan and laurdan in SUVs composed of DPPC at 25 °C and 50 °C, i. e., temperatures below and above their respective main phase transition temperature, at different concentrations of the phospholipid membrane. The emission spectra of both dyes possess two bands, e. g., the short-wavelength band ($\lambda_{max} = 440$ nm, blue band) attributed to the normal fluorescence $S_1(LE) \rightarrow S_0$ and the long-wavelength ($\lambda_{max} = 490$ nm, green band) ascribed to the $S_1(CT) \rightarrow S_0$ charge-transfer emission. Thus, the luminescence probes consist of two ensembles of emitting molecules simultaneously existing in the $S_1(LE)$ or $S_1(CT)$ states. The individuality of these molecules is best manifested in the luminescence spectra and fluorescence decay times [6, 14 – 16]. In the gel phase (at 25 °C) the emission spectrum of prodan at higher lipid concentration possesses the distinct band structure which appears to be broadened in the liquid-crystalline phase (at 50 °C). It is important to note, that the fluorescence spectrum of laurdan does not change its shape with increasing concentration of lipids and, at 50 °C, it is shifted to longer wavelengths compared to the gel phase. It is a consequence of relative intensity changes of the F(LE) and F(CT) bands. Its relative intensities depend on the phase state of the membrane and, in the case of prodan, on the concentration of lipid in the solution. The fit of the experimental spectra with two symmetrical Gaussian bands, demonstrated in Fig. 2, confirm the above statements for prodan and laurdan molecules in both phase states.

The separated bands, named, respectively, locally excited fluorescence band (LE, $\lambda_{max}^{LE} = 440$ nm) and charge-transfer fluorescence band (CT, $\lambda_{max}^{CT} = 490$ nm), are emitted from ensembles of the molecules with the plane of the $-N(CH_3)_2$ group parallel and perpendicular to that of the naphthalene moiety [15]. The conformational transition from the LE configuration to the TICT configuration is accompanied by strong changes in the luminescence spectra (Figs. 1 and 2).

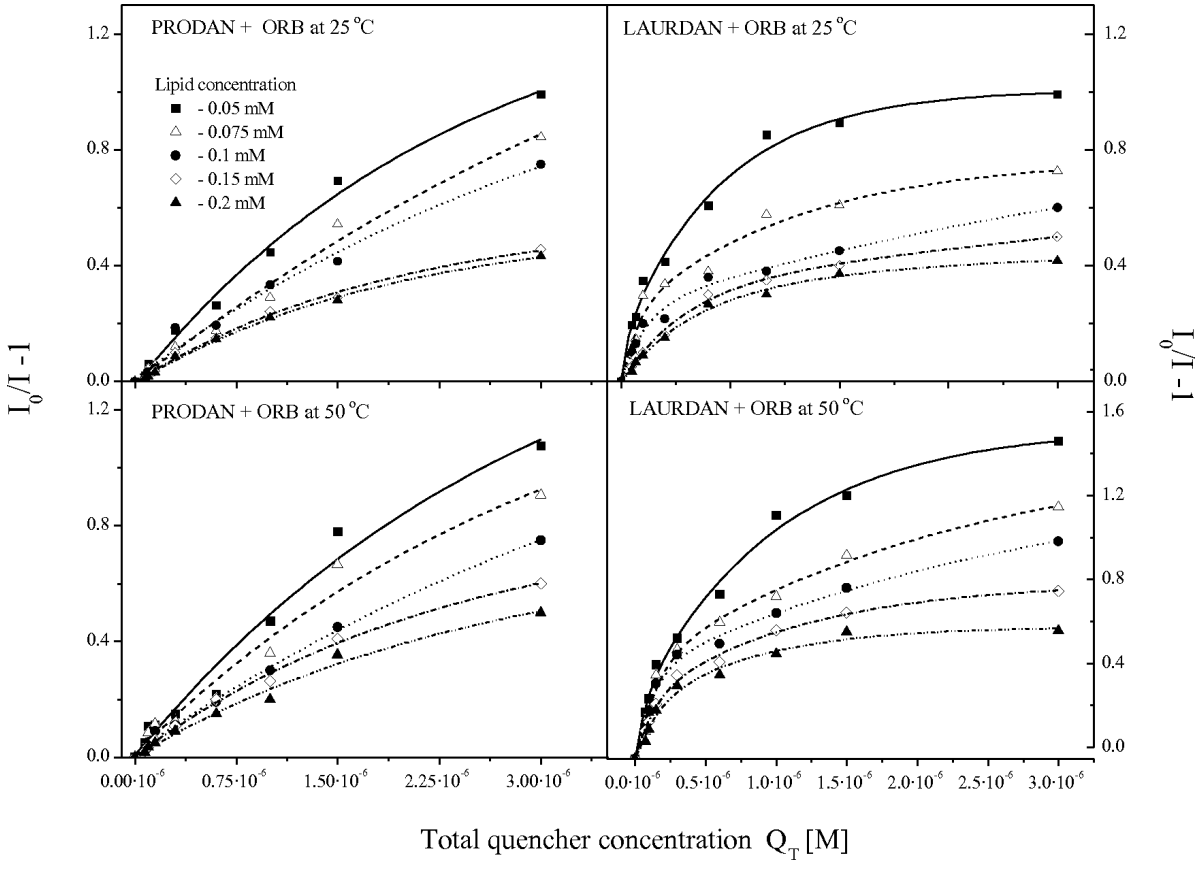

Fig. 4. Stern-Volmer plots of the fluorescence quenching of prodan and laurdan in DPPC liposomes using ORB as a quencher as a function of the lipid concentration.

These findings indicate that prodan and laurdan in SUVs composed of DPPC establish an inhomogeneous spectroscopic medium in both phase states. In fact, the increase of the solvent temperature increases the mobility of the dimethylamino group, causing radiationless transitions $S_1(LE) \rightarrow S_1(CT)$ of both molecules.

It is expected that this spectral heterogeneity and the observed changes of the fluorescence spectra due to the phase transition of the phospholipid vesicles should affect the fluorescence quenching phenomena.

3.2. Fluorescence Quenching

As can be seen in Fig. 2, the fluorescence spectra [whole and separated F(LE) and F(CT) band] of prodan and laurdan significantly overlap the absorption spectrum of the quencher ORB, i. e., the resonance conditions required for a remote dipole-dipole excitation energy transfer from prodan and laurdan to ORB are provided. Thus it seems probable that the membrane-associated donor fluorescence quenching by incorporated acceptor molecules is due to an inductive resonance energy transfer [6, 14]. Figure 3 shows exemplary fluorescence spectra of prodan (panels A, A′) and laurdan (panels B, B′) in DPPC vesicles (lipid concentration 2 mM) determined at 25 °C (gel phase) and 50 °C (liquid-crystalline phase) as a function of the ORB concentration. The inserts in each panel show the very weak fluorescence spectrum of ORB with an intensity one order smaller than that of prodan and laurdan fluorescence; thus it is neglected in our discussion. As can be noticed the intensity of the fluorescence spectra of laurdan and prodan decrease with increasing ORB concentration, whereas the emission of the quencher increases.

Figure 4 shows typical Stern-Volmer plots obtained for different lipid concentrations which result in the dilution of the donor and acceptor concentration. The

Table 1. Stern-Volmer constants, K_{SV}^{LE} and K_{SV}^{CT}, rate constants of fluorescence quenching, k_{ET}^{LE} and k_{ET}^{CT}, and fractional contributions of the emitting forms being in the $S_1(LE)$ and $S_1(CT)$ states to the total fluorescence intensity, f_{LE} and f_{CT}, obtained by means of (1) for the prodan-ORB system in DPPC.

Temperature	[L] [mM]	f_{LE}	K_{SV}^{LE} [l mol^{-1}]	τ_D^{LE} [ns]	k_{ET}^{LE} [10^{11} l mol^{-1} s^{-1}]	f_{CT}	K_{SV}^{CT} [l mol^{-1}]	τ_D^{CT} [ns]	k_{ET}^{CT} [10^{11} l mol^{-1} s^{-1}]
25 °C	0.05	0.54	174	0.85	2.0	0.46	1663	6.40	2.6
	0.075	0.56	322	0.67	4.8	0.44	1174	6.26	1.8
	0.1	0.59	217	0.36	6.0	0.41	2513	6.44	3.9
	0.15	0.66	129	0.29	4.4	0.34	3972	6.32	6.3
	0.2	0.61	192	0.69	2.8	0.39	4218	6.52	6.4
50 °C	0.05	0.61	340	0.84	4.0	0.39	2593	4.86	5.3
	0.075	0.68	331	0.59	5.6	0.32	2911	4.53	6.4
	0.1	0.71	258	0.65	3.9	0.29	3362	4.53	7.4
	0.15	0.62	320	0.38	8.4	0.38	5517	3.80	14.5
	0.2	0.62	320	0.64	5.0	0.38	5671	4.16	13.6

Table 2. Stern-Volmer constants, K_{CV}^{LE} and K_{SV}^{CT}, rate constants of fluorescence quenching, k_{ET}^{LE} and k_{ET}^{CT}, and fractional contributions of the emitting forms being in the $S_1(LE)$ and $S_1(CT)$ states to the total fluorescence intensity, f_{LE} and f_{CT}, obtained by means of (1) for the laurdan-ORB system in DPPC.

Temperature	[L] [mM]	f_{LE}	K_{SV}^{LE} [l mol^{-1}]	τ_D^{LE} [ns]	k_{ET}^{LE} [10^{11} l mol^{-1} s^{-1}]	f_{CT}	K_{SV}^{CT} [l mol^{-1}]	τ_D^{CT} [ns]	k_{ET}^{CT} [10^{11} l mol^{-1} s^{-1}]
25 °C	0.05	0.50	31		0.4	0.50	7554		1.0
	0.075	0.72	112		1.5	0.28	13692		2.0
	0.1	0.73	76	0.75	1.0	0.27	7905	6.95	1.1
	0.15	0.69	65		0.8	0.31	11411		1.6
	0.2	0.68	55		0.7	0.32	13588		1.9
50 °C	0.05	0.44	129		2.5	0.56	11999		3.9
	0.075	0.51	165		3.2	0.49	17604		5.8
	0.1	0.58	261	0.51	5.1	0.42	30770	3.03	10.1
	0.15	0.58	168		3.3	0.42	31126		10.2
	0.2	0.60	73		1.4	0.40	38371		12.6

plots of fluorescence intensity ratio in the absence (I_0) and presence of acceptor (I), I_0/I, versus quencher concentration ([Q]) show a negative deviation from linearity for all studied donor-acceptor pairs at both temperatures: 25 and 50 °C.

On the basis of fluorescence spectra studies and our previous works [6, 14, 15, 20, 22], prodan and laurdan in solution form an inhomogeneous spectroscopic medium in which multi-channel luminescence phenomena take place. Taking this into account, the modified form of the Stern-Volmer relation have been used for analyzing the fluorescence quenching data shown on Fig. 4 [2, 3, 23]. Denoting the emitting forms of donor molecules as $S_1(LE)$ and $S_1(CT)$, the quantitative expression for the relation between fluorescence intensity and quencher concentration is given by the equation [2, 3, 23]

$$\frac{I}{I_0} = \frac{f_{LE}}{1+K_{SV}^{LE}[Q]} + \frac{f_{CT}}{1+K_{SV}^{CT}[Q]} = \frac{f_{LE}}{1+\tau_D^{LE}k_{ET}^{LE}[Q]} + \frac{f_{CT}}{1+\tau_D^{CT}k_{ET}^{CT}[Q]}, \quad (1)$$

where I_0 and I denote the total fluorescence intensities of a fluorophore in the absence and presence of the quencher, respectively. f_{LE} and f_{CT} are the fractional contributions of the emitting forms to the total fluorescence intensity, K_{SV}^{LE}, K_{SV}^{CT}, k_{ET}^{LE}, k_{ET}^{LE}, τ_D^{LE} and τ_D^{CT} are the Stern-Volmer constants, fluorescence quenching rate constants and decay times of emitting forms, respectively.

The fitting of experimental data to (1) was performed by using a non-linear least-squares procedure (ORIGIN 7.0). As a result of performed calculations the values of K_{SV}^{LE}, K_{SV}^{CT}, f_{LE} and f_{CT} were obtained. Using the Stern-Volmer constants (K_{SV}^{LE} and K_{SV}^{CT}) and experimentally determined decay times (τ_D^{LE} and τ_D^{CT}), the energy transfer rate constants (k_{ET}^{LE} and k_{ET}^{CT}) for prodan and laurdan molecules emitted from $S_1(LE)$ and $S_1(CT)$ states were calculated. The results are listed in Tables 1 and 2. An accurate analysis of the parameters describing the fluorescence quenching of the studied D-A pairs indicates that:

- the values of k_{ET}^{LE} and k_{ET}^{CT} for prodan-ORB and

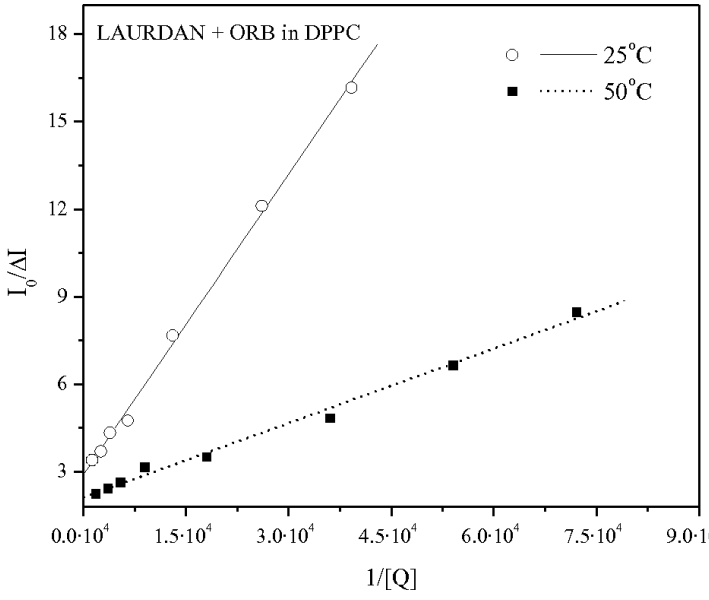

Fig. 5. Plot of $I_0/\Delta I$ versus 1/[Q] for the laurdan-ORB system in a phospholipid membrane.

laurdan-ORB systems comprise $0.4 \cdot 10^{11} - 2.0 \cdot 10^{12}$ l mol^{-1} s^{-1} and depend on the lipid concentration. For all studied systems the k_{ET}^{LE} and k_{ET}^{CT} values increase with increasing the lipid concentration. For some lipid concentrations the values of k_{ET}^{LE} and k_{ET}^{CT} change irregular.

• the membrane phase transition from a gel to a liquid-crystalline state causes an increase of all k_{ET} values, e. g., for the prodan-ORB system: k_{ET}^{LE} (25 °C) $= 2.0 \cdot 10^{11}$ l mol^{-1} s^{-1} and k_{ET}^{LE} (50 °C) $= 4.0 \cdot 10^{11}$ l mol^{-1} s^{-1}, and k_{ET}^{CT} (25 °C) $= 2.6 \cdot 10^{11}$ l mol^{-1} s^{-1} and k_{ET}^{CT} (50 °C) $= 5.3 \cdot 10^{11}$ l mol^{-1} s^{-1}. It also causes that the emission arising from molecules in the S_1(LE) state is more effectively quenched than that from the S_1(CT) state. An opposite situation is observed for the laurdan-ORB system.

• the values of f_{LE} and f_{CT} agree well with the values of A_i describing contributions from different fluorescence emitting modes determined in our previous work [16], e. g., for prodan-ORB in DPPC at 50 °C: $f_{LE} = 0.68$ and A_1(LE) $= 0.71$, and $f_{CT} = 0.32$ and A_2(CT) $= 0.29$, while for laurdan, the following results were obtained: $f_{LE} = 0.51$ and A_1(LE) $= 0.53$, and $f_{CT} = 0.49$ and A_2(CT) $= 0.47$.

In addition, the non-linear Stern-Volmer plots have been analyzed using the theory proposed by Lehrer [7]. According to Lehrer, there are some emitting centres which do not participate in the quenching process. The relation between the donor fluorescence intensity and the quencher concentration in case where the fluorophores have different accessibility to fluorescence quenching is given by the equation

$$\frac{I_0}{\Delta I} = \frac{1}{f_a K_{SV,a}[Q]} + \frac{1}{f_a}, \qquad (2)$$

where $\Delta I = I_0 - I$, and f_a is a fraction of donor molecules that are accessible to the quenching process, and $K_{SV,a}$ is the quenching constant for this accessible assembles. From the intercept and slope of the linear plot $I_0/\Delta I$ versus $1/[Q]$, the f_a and $K_{SV,a}$ values can be determined. It should be noted that (2) is valid, if we suppose that two emitting forms of donor molecules, S_1(LE) and S_1(CT), are quenched with the same probability [7].

In many systems, particularly in those involving membranes or micelles, the luminescent probes may be partitioned between the aqueous phase and the lipid phase [24]. Because of different lengths of the prodan and laurdan alkyl residues, the two probe molecules are located differently in the bilayer, and their affinities for the different membrane phase domains are predominantly different. In phospholipid bilayers laurdan is tightly anchored in the hydrophobic core and is virtually insoluble in water. The observed emission originates entirely from probes within the phospholipid environment. Prodan with its shorter propionyl tail is more loosely anchored in the bilayer and has a higher water solubility [24, 25]. Assuming that only fluorescence of the molecules in the phospholipid environ-

Table 3. Stern-Volmer constants for accessible assembles, $K_{SV,a}$, rate constants of fluorescence quenching, k_q, and fraction of donor molecules that are accessible to the quenching process, f_a, obtained by means of (2) for the prodan-ORB and laurdan-ORB systems in DPPC.

System	[L] [mM]	Temperature 25 °C f_a	$K_{SV,a}$ [l mol^{-1}]	$\langle\tau\rangle^*$ [ns]	k_q [10^{11} l mol^{-1} s^{-1}]	Temperature 50 °C f_a	$K_{SV,a}$ [l mol^{-1}]	$\langle\tau\rangle^*$ [ns]	k_q [10^{11} l mol^{-1} s^{-1}]
Prodan + ORB	0.05	0.62	1295	4.55	2.84	0.50	2572	1.57	1.64
	0.075	0.46	1885	4.46	4.22	0.64	1926	1.90	1.00
	0.1	0.86	957	4.24	2.25	0.70	1553	1.73	0.91
	0.15	0.78	1294	4.25	3.04	0.59	3401	2.60	1.30
	0.2	0.89	1330	4.57	2.91	0.56	3524	2.65	1.33
Laurdan + ORB	0.05	0.50	8097		1.28	0.61	10353		3.34
	0.075	0.48	2414		0.38	0.65	8917		2.87
	0.1	0.34	5628	6.30	0.89	0.52	19428	3.10	6.26
	0.15	0.34	8508		1.35	0.47	24892		8.03
	0.2	0.34	11255		1.79	0.52	18982		6.12

* Calculated using the formula: $\langle\tau\rangle = \sum_i A_i\tau_i^2 / \sum_i A_i\tau_i$, where the τ_i and A_i data are taken from [6].

ment is quenched, the fraction of molecules participating in the quenching process can be estimated using (2).

Figure 5 shows a linear dependence of $I_0/\Delta I$ as a function of $1/[Q]$ for the laurdan-ORB system in DPPC for the lipid concentration $[L] = 0.15$ mM as required in (2). As it can be seen, this dependence is linear for both a gel and liquid-crystalline phase of the membrane and is observed under all experimental conditions for all lipid concentrations of both D-A under study. Fitting the experimental data to (2), the values of f_a and $K_{SV,a}$ are obtained (listed in Table 3). Using the equation $K_{SV,a} = k_q\langle\tau\rangle$ and averaging the values of the fluorescence decay time from the three fluorescence modes $\langle\tau\rangle$ (they are taken from [6] and assembled in Table 3), the fluorescence quenching rate constant of accessible components k_q can be calculated. On analyzing the results listed in Table 3, we can state that:

- the number of molecules participating in the fluorescence quenching process increases with increasing lipid concentration.
- the values of f_a depend on a membrane phase state, i. e., for prodan $f_a\,(25\ ^\circ\mathrm{C}) > f_a\,(50\ ^\circ\mathrm{C})$. In contrast to prodan, laurdan demonstrates the opposite behaviour, i. e. $f_a\,(25\ ^\circ\mathrm{C}) < f_a\,(50\ ^\circ\mathrm{C})$. This difference noted for both probes is a consequence of their hydrophobic differences caused by different lengths of the aliphatic $-(CH_2)_n$ groups.

3.3. Resonance Excitation Energy Transfer

Fluorescence quenching can be a result of the resonance excitation energy transfer, due to dipole-dipole interactions between donor D and acceptor A molecules. In our previous work [6], where prodan and laurdan have been used as donors in the studies of fluorescence quenching by ORB, factors determining the energy transfer process [spectral overlap integral $J_{DA}(\tilde{\nu})$, a critical distance for the energy transfer R_0] were calculated using the Förster theory [26]. As it was mentioned earlier, the proper description of the energy transfer process in a membrane requires consideration of such factors as in the model of the acceptor bilayer distribution, the curvature of lipid-water interface, the extent of area exclusion around fluorophore. The study of non-radiative energy transfer in a lipid bilayer is based on measurements of the efficiency of this process as a function of the acceptor surface density.

Figure 6 shows a scheme of small spherical unilamellar lipid vesicles and the expected localization of donor (prodan, laurdan) and acceptor (ORB) molecules in the liposomal bilayer [15]. The efficiency of the energy transfer (E_T) in such a membrane is the function of the mutual distance between donor D and acceptor A molecules (r_{DA}) and surface concentration of acceptor molecules (σ_a). According to Frolov et al. [13], E_T can be calculated using the formula

$$E_T = 1 - \frac{\Phi^D}{\Phi_0^D} = 1 - \left[1 + \sigma_A R_0^6 \left\langle \frac{1}{r_{DA}^6} \right\rangle\right]^{-1} . \quad (3)$$

Therefore to calculate the efficiency of the resonance excitation energy transfer E_T of such a statistical ensemble according to (3), it is necessary to use the average value of $\langle 1/r_{DA}^6\rangle$ determined from the distribution of D and A molecules in the vesicle. If the D molecule is situated in the spherical layer at a distance between

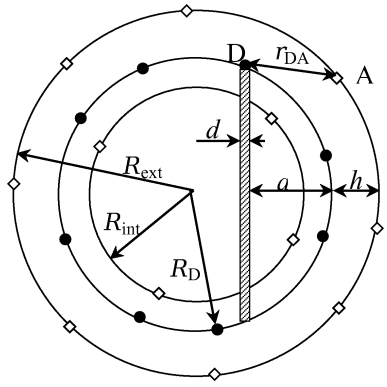

Fig. 6. Scheme of a small unilamellar lipid vesicle (SUV) and assumed localization of donor (D) and acceptor (A) molecules in the lipid bilayer. R_{int} and R_{ext} are the internal and external radii of the SUV, respectively, R_D is the radius of localization of the D molecules, r_{DA} is the distance between D and A, h is the average distance of D localization from the outer surface of the SUV, and a is the spherical segment height.

a (a is the segment height) and $(a+\mathrm{d}a)$ (see Fig. 6), then the area of this layer $(2\pi \mathrm{R_D d}a)$ characterizes the probability of finding donor molecules in this layer. Hence, if r_{DA} is the distance from a molecule A to any molecule D in this spherical layer, we obtain the following expression for the mean value of $\langle 1/r_{DA}^6 \rangle$ [15]:

$$\left\langle \frac{1}{r_{DA}^6} \right\rangle = \frac{\int_0^{2R_D} 2\pi R_D \mathrm{d}a / r_{DA}^6}{\int_0^{2R_D} 2\pi R_D \mathrm{d}a} = \frac{1}{8R_D(R_D+h)} \left\{ \frac{1}{h^4} - \frac{1}{[4R_D(R_D+h)+h^2]^2} \right\}. \quad (4)$$

The distribution of ORB molecules on the membrane surface during incorporation into the vesicles from the aqueous phase is known [27]. Because of their electric charge ORB molecules are adsorbed at the water-lipid interface and anchored to the vesicles via the lipophilic C_{18} alkyl chain. Assuming that D and A molecules are uniformly distributed and fixed on spheres of different radii (R_D and R_{ext}), and that A molecules are distributed only over the external half on the bilayer, the theoretical curves for prodan and laurdan fluorescence quenching can be calculated using (3). For determination of the surface acceptor concentration (σ_A) for the DPPC polar head areas in the gel and liquid-crystalline phases, respectively, the values of 52.3 and 72.1 Å^2 were assumed [28].

Table 4. Experimentally and theoretically determined values of the critical energy transfer distance, R_0, radius of the localization of D molecules, R_D, and average distance of D localization from the outer surface of SUV, h, for the prodan-ORB and laurdan-ORB systems.

Donor	T [°C]	Φ_D^0	$J_{DA}(\tilde{\nu})$ [10^{-11} cm^6 mol^{-1}]	R_0 [Å]	R_D [Å]	h [Å]
Prodan	25	0.23	5.870	108.3	139	11
	50	0.14	6.131	100.2	141	9
Laurdan	25	0.60	1.252	98.0	138	12
	50	0.52	4.075	116.5	138	12

Figure 7 shows a family of theoretical curves describing the energy transfer efficiency calculated using (3). The values of $\langle \frac{1}{r_{DA}^6} \rangle$ have been obtained using (4) by varying the values of R_D and h (see legend of Fig. 7). The possible limits for R_D and h were chosen by considering the size of model membranes ($R = 150$ Å determined by experimental preparation of a membrane composed of DPPC). Additionally, the limit for h, which determines the average distance of D molecules localization from the outer surface of a SUV, was confined to the size of the hydrophilic region of the bilayer. The points in Fig. 7 represent our experimental results.

Analyzing the families of E_T curves given in Fig. 7, it follows that the transition to the liquid-crystalline phase results in a considerable lateral expansion of the bilayer and decreased lipid order in the region of the hydrophobic chains. Otherwise, the thickness of the hydrophilic region changes with the temperature, and equals 16.7 Å and 11.8 Å for 25 °C and 50 °C, respectively [29]. The estimation of R_D and h requires consideration of the fact that prodan and laurdan are localized in the hydrophilic region of the bilayer. Thus, the values of h cannot exceed the value of the thickness of the hydrophilic region.

Table 4 collects the values of R_D and h for which the empirical points are in good agreement with theoretical calculations. From our studies it follows that R_D and h are independent of the lipid concentration. Notwithstanding, as it can be noted for laurdan, h depends on the phase state of the membrane. Furthermore, it can be seen, that the spatial macrolocalization of the used fluorophores in SUVs is different, i. e. laurdan molecules are localized more deeply in the bilayer than prodan molecules do.

4. Conclusions

A detailed electronic energy transfer study between donor (prodan and laurdan) and acceptor (ORB)

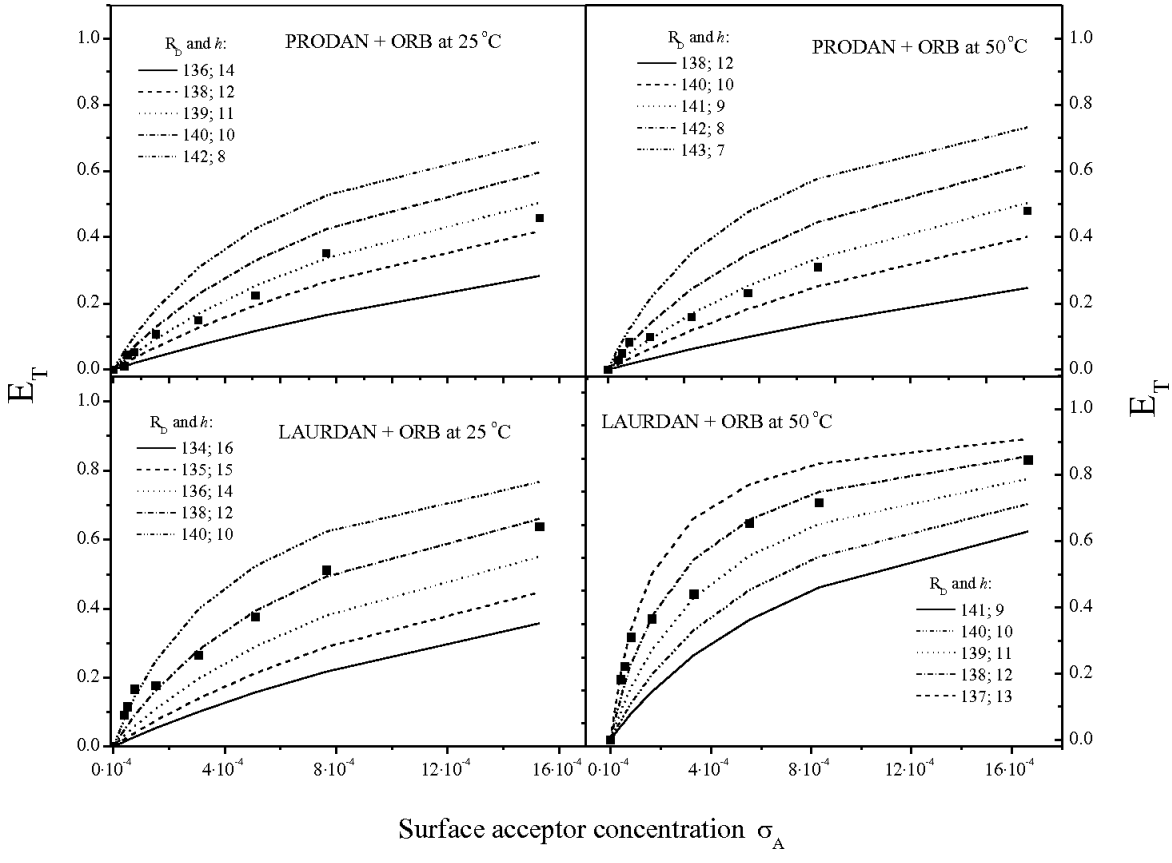

Fig. 7. Prodan and laurdan fluorescence quenching by ORB in a liposome bilayer (C_D = const.). The full and dashed curves are calculated by means of (3). The squares represent our experimental data.

molecules solubilized in small unilamellar vesicles of DPPC in the gel and liquid-crystalline phases has been carried out. The relative quenching efficiencies of prodan and laurdan depend on the phase state of the bilayer and are higher for the liquid-crystalline phase. This result is reasonable because of a greater mobility of D molecules in the liquid-crystalline compared to the gel phase bilayer. Otherwise, consideration of the spectral heterogeneity of prodan and laurdan in the phospholipid membrane led to the finding that the emission arising from $S_1(LE)$ and $S_1(CT)$ states is quenched with different efficiencies, and in the case of the prodan-ORB system the $S_1(LE)$ state is more effectively quenched than the $S_1(CT)$ state, in contrast to the laurdan-ORB system.

The results of the performed studies indicate that fluorescence quenching of prodan and laurdan due to the resonance energy transfer to ORB molecules incorporated into the lipid bilayer can be used as a methodological approach to obtain a more definite substantiation of the spatial macrolocalization of luminescent probes in SUVs. A set of parameters employed in the data analysis involves a distance of the donor localization from the outer surface of a SUV (h), which is equivalent to the distance of the closest approach between donor and acceptor molecules. Varying R_D and h in the limits, consistent with the model membranes, yields possible limits for the donor distance from the lipid bilayer surface and the depth of penetration into the membrane interior. The obtained emission spectra and fluorescence quenching data suggest that the incorporation of prodan and laurdan is deeper in the fluid phase than in the gel phase of the membrane.

Acknowledgements

The authors express their gratitude to Prof. Dr. H. A. Diehl and Dr. M. Engelke for their help in preparation

of phospholipid membranes. This work is in part supported by the KBN grant 127/E-335/S/2004, the funding scientific co-operation between the University of Gdansk and the University of Bremen.

[1] P. Wu and L. Brand, Anal. Biochem. **218**, 1 (1994).
[2] T. G. Dewey (Ed.), Biophysical and Biochemical Aspects of Fluorescence Spectroscopy, Plenum Press, New York 1991.
[3] J. R. Lakowicz (Ed.), Topics in Fluorescence Spectroscopy: Principles, Plenum Press, New York 1991.
[4] J. R. Lakowicz, Principles of Fluorescence Spectroscopy, Kluwer Academic Publishers, New York 1999.
[5] O. Stern and M. Volmer, Phys. Z. **20**, 183 (1919).
[6] K. A. Kozyra, J. R. Heldt, M. Engelke, and H. A. Diehl, Spectrochim. Acta A **61**, 1153 (2005).
[7] S. S. Lehrer, Biochemistry **10**, 3254 (1971).
[8] L. M. S. Loura, A. Fedorov, and M. Prieto, Biophys. J. **71**, 1823 (1996).
[9] B. Fung and L. Stryer, Biochemistry **17**, 5241 (1978).
[10] T. Estep and T. Thompson, Biophys. J. **26**, 195 (1979).
[11] P. Wolber and B. Hudson, Biophys. J. **28**, 197 (1979).
[12] B. Snyder and E. Freire, Biophys. J. **40**, 137 (1982).
[13] A. A. Frolov, E. I. Zenkevich, G. P. Gurinovich, and G. A. Kochubeyev, J. Photochem. Photobiol. B **7**, 43 (1990).
[14] K. A. Kozyra, J. R. Heldt, G. Gondek, P. Kwiek, and J. Heldt, Z. Naturforsch. **59a**, 809 (2004).
[15] M. Brozis, K. A. Kozyra, V. I. Tomin, and J. Heldt, J. Appl. Spectrosc. **69**, 480 (2002).
[16] M. Józefowicz, K. A. Kozyra, J. R. Heldt, and J. Heldt, Chem. Phys. **320**, 45 (2005).
[17] G. Duportail, F. Merola, and P. Lianos, J. Photochem. Photobiol. A **89**, 135 (1995).
[18] R. Hutterer, F. W. Schneider, H. Sprinz, and M. Hof, Biophys. Chem. **61**, 151 (1996).
[19] L. M. S. Loura, A. Fedorov, and M. Prieto, Biophys. J. **80**, 776 (2001).
[20] K. A. Kozyra, J. R. Heldt, and J. Heldt, Biophys. Chem. **121**, 57 (2006).
[21] R. R. C. New (Ed.), Liposomes: A Practical Approach, Oxford University Press, New York 1990.
[22] K. A. Kozyra, J. R. Heldt, J. Heldt, M. Engelke, and H. A. Diehl, Z. Naturforsch. **58a**, 581 (2003).
[23] B. Valuer, Molecular Fluorescence, Wiley-VCH, Weinheim 2002.
[24] E. K. Krasnowska, E. Gratton, and T. Parasassi, Biophys. J. **74**, 1984 (1998).
[25] T. Parasassi, E. K. Krasnowska, L. Bagatolli, and E. Gratton, J. Fluoresc. **8**, 365 (1998).
[26] T. Förster, Disc. Faraday Soc. **27**, 7 (1959).
[27] L. B. A. Johansson and A. Niemi, J. Phys. Chem. **91**, 3020 (1987).
[28] D. Marsh, Handbook of Lipid Bilayers, CRC Press, Boca Raton 1990.
[29] A. Continho, J. Costa, J. L. Faria, M. N. Berberan-Santos, and M. J. E. Prieto, Eur. J. Biochem. **189**, 387 (1990).